XLI CILAMCE
XLI Ibero-Latin American Congress on Computational Methods in Engineering
16-19 November, 2020 FOZ DO IGUAÇU PARANÁ - BRAZIL

Poroelastic Modeling of Piezocone Tests Using Poroelastic Cavity Expansion Analysis

Vicente Mafra[1], Gracieli Dienstmann[2]

[1]*Dept. of Civil Engeneering, Federal University of Santa Catarina – UFSC.*
Florianópolis, Santa Catarina, Brazil
vicentemafra42@gmail.com
[2]*Dept. of Civil Engeneering, Federal University of Santa Catarina – UFSC.*
Florianópolis, Santa Catarina, Brazil
g.dienstmann@ufsc.br

Abstract. The CPTu (Cone Penetration Test with pore pressure measurements) is a field test widely used to obtain stratigraphic characterization and geotechnical properties of a subsoil profile. In general, the speed used for driving the cone is standardized at 20 mm/s. In this way, predominantly sandy soils tend to show drained behavior, in such manner the analysis is based on effective tensions; and predominantly clayey soils tend to show undrained behavior, thus the analyze is based on total stresses. In this sense, classical methods of interpretation are set to define with an accepted reliability behavior of typical sands or clays. However, for mixtures or silty soils, drainage may be partial. In this condition, the pore pressure around the cone is altered introducing errors in the interpretation. The present work aims to present a model capable to identify the drainage behavior of soils submitted to CPTu with intermediate permeability characteristics (silty soils). To evaluate the drainage behavior during the execution of the test, simplified semi-analytical models of cylindrical cavity expansion were developed, based on the theories of poroelasticity presented by Biot [1]. Preliminary results indicate that the model has the capacity to evaluate the typical drainage behavior of the soil submitted to CPT.

Keywords: cavity expansion, CPT, poroelasticity.

1 Introduction

The CPT(Cone penetration Test) is a field test, it is used to obtain typical soil behaviors and stratigraphic characterization (Coutinho e Mellia [2]). This test is based on the resistance developed by the soil against a driving conical tip. Usually, the speed normalized by ASTM [3] and ABNT [4] of 20 mm/s is used. The soil resistance is measured by load cells connected to the conical tip and a friction sleeve. Additionally, pore pressure sensors can be installed in the equipment.

According to Schnaid and Odebrecht [5], the CPTu and the classical interpretation approach were developed based mainly in sandy or clay deposits, known as conventional materials. Thus, other materials may require a different test or interpretation procedure. Materials with intermediate permeability, such as silts for example, are not included in the classic methods of interpretation. These materials usually present partial drainage during the execution of the standard CPTu, which makes the classical approach interpretation inappropriate considering the assumptions of drainage conditions: drained or undrained. Thus, it can be said that the knowledge of the drainage condition during the execution of the CPTu is essential to guarantee the reliability of the test results, as stated by many authors.

Schnaider et al. [6], through small scale tests, states that the interpretation of CPTu results obtained in partial drainage conditions is not reliable. DeJong and Randolph [7] describe that the interpretation of the consolidation coefficient may contain errors by one order of magnitude under these conditions. Considering the difficulty in interpreting the test under conditions of partial drainage, Salgado and Prezzi [8] suggest to vary the rate of penetration to guarantee that the test is executed in a fully drained or undrained condition.

In order to access the drainage condition in vane tests Blight [9] introduces the concept of degree of drainage, a relationship between the resistances obtained by the completely drained and completely undrained condition. By relating this quantity to the velocity of the test, a characteristic drainage curve is obtained.

When adopted for cone tests, the concept of characteristic drainage curves, is presented by the relating of a normalized penetration rate (V) with a normalized penetration resistance (Q) or normalized drainage (U) (*e.g.* Schneider *et al.* [6]; Dejong and Randolph [7]; Dienstmann [10]; Forcelini [11]; Kim *et al*. [12]; Chung *et al.* [13]; Suzuki and Lehane [14]). In particular, the normalized rate V is generally described as

$$V=\frac{v\cdot d}{C_i} \tag{1}$$

where v is the penetration rate, d is the diameter of the cone tip C_i is a coefficient of consolidation: vertical (C_v) or horizontal (C_h).

Further, U [eq. 2] and Q [eq. 3] are the normalized pore pressure (u_2) and resistance (q_c) in relation to initial stress (σ_0) and initial pore pressure (u_0), respectively.

$$U=\frac{u_2-u_0}{u_0} \tag{2}$$

$$Q=\frac{q_c-\sigma_0}{\sigma_0} \tag{3}$$

In order to evaluate the mechanisms related to soil drainage response in the CPTu, this article presents a numerical model of cavity expansion, related to that presented by Dienstmann [10] and based on the theory of poroelasticity presented by Biot [1] and aims to characterize theoretical drainage curves according to the material characteristics.

2 Model description

The model presented simulates the expansion of a cylindrical cavity embedded by a mass of non-linear, isotropic and saturated poroelastic soil. The Drucker-Prager criterion was linked to the material. Results of radial distribution of pore pressure, stresses and deformations are obtained from the model as a result of semi-analytical solutions. Figure 1 shows the representation of the cavity expansion model: the cylinder wall, with initial radius R and the imposed displacement (ξ), with size related to the radius on the face of the cylinder ($\alpha\cdot R$). The analyzes is based on plane strains, with flow and displacements in the radial direction.

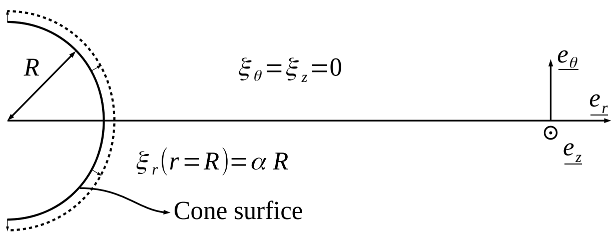

Figure 1. Model graphic layout

2.1 Poroelastic problem

The poroelastic problem, as described by Biot [1], is the composition of a solid matrix and a porous medium. The solid matrix respects the elasticity and the fluid medium a flow law (general Darcy law of flow is considered). In this context, the Biot coefficient (b) and the Biot modulus (M)

$$b=1-\frac{K}{K_s} \quad and \quad \frac{1}{M}=\frac{1}{N}+\frac{\Phi_0}{K_w}, \tag{4}$$

where

$$N = \frac{b - \Phi_0}{K_s} \tag{5}$$

establish the relationship between the porosity variation (Φ_0), the soil volumetric modulus (K), the soil solids volumetric modulus (K_s) and the fluid volume modulus (K_w).

Regarding the flow laws, the relationship between the mass flow ($\underline{w}$) and the pore pressure excess gradient (∇u) is expressed by the hydraulic conductivity ($\underline{\underline{k}}$):

$$\underline{w} = -\rho_w \underline{\underline{k}} \cdot (\nabla u) \tag{6}$$

where ρ_w is the fluid mass density. Additionally, a mass conservation relationship can be described, which relates the rate of variation of the porosity in relation to time with the mass flow gradient:

$$\rho_w \cdot \frac{\partial \Phi}{\partial t} = \nabla \cdot \underline{w} \tag{7}$$

Replacing the content of eq. 7 in eq. 6, eq. 8 is reached:

$$\frac{\partial (\Delta \Phi)}{\partial t} + \underline{\underline{k}} \cdot \nabla^2 u = 0 \tag{8}$$

where ∇^2 is the Laplacian operator. Furthermore, considering $\underline{\underline{k}} \cdot \nabla u = \underline{q}$, eq. 8 can be rewritten as

$$\frac{\partial (\Delta \Phi)}{\partial t} + \nabla \underline{q} = 0. \tag{9}$$

Regarding elasticity, Biot [1] describes, in a comprehensive way, the relationship between the variation of the stress with the deformation and the pore pressure variation:

$$\Delta \underline{\underline{\sigma}} = \underline{\underline{\underline{\underline{C}}}} : \underline{\underline{\varepsilon}} - \underline{\underline{B}} \cdot \Delta u \tag{10}$$

In the isotropic case, the elastic matrix ($\underline{\underline{\underline{\underline{C}}}}$) can be replaced by the Lamé parameters (λ and G) and the Biot tensor ($\underline{\underline{B}}$) can be replaced by the Biot coefficient (b),

$$\Delta \underline{\underline{\sigma}} = \lambda \cdot tr \, \underline{\underline{\varepsilon}} + 2G \cdot \underline{\underline{\varepsilon}} - b \cdot \Delta u \cdot \underline{\underline{1}}, \tag{11}$$

resulting in the first equation of the poroelastic medium. In addition, to define the second equation of the poroelastic medium, the porosity variation

$$(\Delta \Phi = \Phi - \Phi_0) \tag{12}$$

can be defined as the function of the trace of the strain tensor ($tr \, \underline{\underline{\varepsilon}}$) and the pore pressure variation:

$$\Delta \Phi = b \cdot tr \, \underline{\underline{\varepsilon}} + \frac{1}{M} \cdot \Delta p \tag{13}$$

In general, the stresses, deformations and pore pressure generated by the cavity expansion have a great influence on the nonlinear behavior of the material. In order to consider this type of behavior to the model, a shear module (G) is adopted as a function of pore pressure (p), volumetric deformation (ε) and the equivalent deviatoric strain (ε_d).

Based on this concept, it seeks to couple the Drucker-Praguer criterion to the material behavior. This yeld criterion may be described by:

$$F(\underline{\underline{\sigma}}') = \sigma_d + T(\sigma'_m - h) \geq 0 \tag{14}$$

where is $\underline{\underline{\sigma}}'$ the effective tension;

$$\sigma_d = \sqrt{(\underline{\underline{\sigma}} - (1/3) tr \, \underline{\underline{\sigma}}) : (\underline{\underline{\sigma}} - (1/3) tr \, \underline{\underline{\sigma}})} \tag{15}$$

is the deviatoric stress;

$$\underline{\underline{\sigma}}'_m = (1/3) \cdot tr \, \underline{\underline{\sigma}} \tag{16}$$

is the mean effective stress; h is the material's friction coefficient and T is the tensile strength following the Drucker-Prager criterion. In this context, Dienstmann [10] extends the ideas presented by Maghous et al. [15], describing a dependency law for G, while the bulk modulus K is kept constant.

$$G = \frac{1}{2} [T(h - K \varepsilon_v - \delta) - \sigma_{0d}] \cdot \frac{1/\varepsilon_{ref}}{1 + \varepsilon_d / \varepsilon_{ref}} \tag{17}$$

where σ_{0d} is the initial deviatoric stress, associated with the initial stress field; ε_{ref} is the reference strain,

$$\varepsilon_d = \sqrt{\left(\underline{\underline{\varepsilon}} - \frac{1}{3} tr \, \underline{\underline{\varepsilon}}\right) : \left(\underline{\underline{\varepsilon}} - \frac{1}{3} tr \, \underline{\underline{\varepsilon}}\right)} \tag{18}$$

is the deviatoric strain and

$$\varepsilon_v = tr\, \underline{\underline{\varepsilon}} \tag{19}$$

is the volumetric strain.

Furthermore, the parameter δ [eq. 17] may be described as

$$\delta = \sigma'_{0m} + (1-b)\cdot\Delta p \tag{20}$$

where σ'_{0m} is the initial mean effective stress. Thus, the behavior asymptotically approaches the Drucker-Prager criterion as can be seen in Fig. 2.

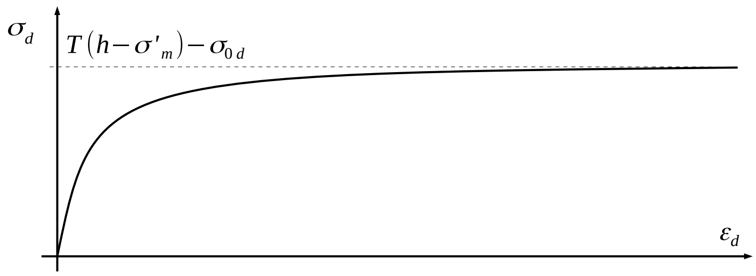

Figure 2. Schematic representation of the asymptotic approximation of elastic behavior associated with the Drucker-Praguer criterion

2.2 Cavity expansion

A simplified poromechanical model based on cylindrical cavity expansion was adopted to represent the driving of the cone into the ground. This model has the premise of being restricted to small deformations. A displacement of dimension αR is imposed on the face of the modeled cavity. This displacement causes a radial displacement field (ξ_{rr}), consequently, radial (ε_{rr}) and tangencial ($\varepsilon_{\theta\theta}$) deformation field. In the longitudinal direction, deformations are restricted, characterizing the plane deformations (Figure 1).

The boundary conditions of displacement of the problem are described for the face of the cylinder (r = R):

$$\xi_r = \alpha R \quad at \quad r = R \quad \forall \quad t > 0 \tag{21}$$

and for all radius (r) greater than the influence zone of the displacements (a_ξ):

$$\xi_r = 0 \quad at \quad r \geq a_\xi \quad \forall \quad t. \tag{22}$$

The displacement field (ξ) is then described as a function of the radius:

$$\underline{\xi} = f(r)\underline{e_r} \tag{23}$$

Also, in view of the adopted cylindrical coordinate system, the radial and tangential deformations can be described in relation to the displacement field (*f(r)*):

$$\underline{\underline{\varepsilon}} = \varepsilon_{rr}(e_r \otimes e_r) + \varepsilon_{\theta\theta}(e_\theta \otimes e_\theta)\, \varepsilon_{rr} = f'(r) \quad \text{with} \quad \varepsilon_{rr} = f'(r) \quad \text{and} \quad \varepsilon_{\theta\theta} = \frac{f(r)}{r} \tag{24}$$

In this way, the deviatoric strain tensor ($\underline{\underline{\varepsilon}}_d$) and its modulus can be written as:

$$\underline{\underline{\varepsilon_d}} = f'(r)(e_r \otimes e_r) + \frac{f(r)}{r}(e_\theta \otimes e_\theta) - \frac{1}{3}\left(f'(r) + \frac{f(r)}{r}\right)\underline{\underline{1}} \tag{25}$$

$$\varepsilon_d = \sqrt{\frac{2}{3}} \cdot \sqrt{f'(r)^2 + \frac{f(r)^2}{r^2} - f'\frac{(r)\cdot f(r)}{r}} \tag{26}$$

The increments of tension,

$$\Delta\underline{\underline{\sigma}} = \lambda\left(f'(r) + \frac{f(r)}{r}\right)\underline{\underline{1}} + 2G\left[\varepsilon_{rr}(e_r \otimes e_r) + \varepsilon_{\theta\theta}(e_\theta \otimes e_\theta)\right] - b\,\Delta p\,\underline{\underline{1}}, \tag{27}$$

are obtained when replacing eq. 24 in the first equation of the elastic medium [eq. 12].

In addition, separating the result into components and using the relationship between Lamé constants and the volumetric deformation moduli (λ = $K - 2G/3$):

$$\Delta\sigma_{rr}=K\left[f'(r)+\frac{f(r)}{r}\right]+\frac{2G}{3}\left[2f'(r)-\frac{f(r)}{r}\right]-b\Delta p \quad (28)$$

$$\Delta\sigma_{\theta\theta}=K\left[f'(r)+\frac{f(r)}{r}\right]+\frac{2G}{3}\left[2\frac{f(r)}{r}-f'(r)\right]-b\Delta p \quad (29)$$

In view of the local stress equilibrium equation,

$$\Delta\sigma_{\theta\theta}=\frac{d}{dr}(r\Delta\sigma_{rr}), \quad (30)$$

eq. 27 can be rewritten as:

$$\frac{d}{dr}\left[K\left(f'(r)+\frac{f(r)}{r}\right)+\frac{2G}{3}\left(2f'(r)-\frac{f(r)}{r}\right)-b\Delta p\right]+\frac{2G}{r}\left(f'(r)-\frac{f(r)}{r}\right)=0 \quad (31)$$

becoming a differential equation that relates the function of displacements (*f(r)*) with the variation in pore pressure (Δp). The development of the problem associated with pore pressure variation is discussed in the next section.

2.3 Flow problem

The solution of the flow problem is dependent on the tension and deformation tensors and is based on the law of mass conservation, as described by Dienstmann [10]. In addition, it is noteworthy that the flow, in the same way as the displacement problem was described, is always described in the radial direction. This solution can be obtained from the derivation in relation to time the second equation of the poroelastic medium [eq. 13] and develop it based on eq. 8 (related to Darcy's law):

$$b\frac{\partial tr\,\underline{\underline{\varepsilon}}}{\partial t}+\frac{1}{M}\cdot\frac{\partial\Delta p}{\partial t}=k\nabla^2 u \quad (32)$$

Additionally, the local equilibrium equation

$$\nabla\cdot\Delta\sigma=0 \quad (33)$$

is applied in the first state equation [eq. 11]:

$$\left[K+\frac{4}{3}G\right]\nabla\, tr\,\underline{\underline{\varepsilon}}-G\nabla\times(\nabla\times\underline{\xi})+2\nabla G\left(\underline{\underline{\varepsilon}}-\frac{1}{3}tr\,\underline{\underline{\varepsilon}}\right)=b\nabla(\Delta p). \quad (34)$$

Considering that the displacement field of the problem is irrotational ($\nabla\times\xi = 0$), eq. 34 can be simplified as:

$$\left[K+\frac{4}{3}G\right]\nabla\, tr\,\underline{\underline{\varepsilon}}+2\nabla G\left(\underline{\underline{\varepsilon}}-\frac{1}{3}tr\,\underline{\underline{\varepsilon}}\right)=b\nabla(\Delta p) \quad (35)$$

The solution of the strain and pore pressure field, therefore, depends on the solution of the system of partial differential equations: [eq. 31, 32 and 35]. However, Dienstmann [10], proposes a solution for decoupled pore pressure, based on the adoption of an equivalent average shear module, which approximates the non-linear shear module that governs the system ($G_{eq} \sim G$), therefore, in this context, eq. 35 can be described as:

$$\left[K+\frac{4}{3}G_{eq}\right]\nabla\, tr\,\underline{\underline{\varepsilon}}=b\nabla(\Delta p) \quad (36)$$

Furthermore, when integrating eq. 36:

$$tr\,\underline{\underline{\varepsilon}}=\frac{b\nabla(\Delta p)}{K+(4/3)G_{eq}}+C(t) \quad (37)$$

where the function *C(t)* must be zero to satisfy the boundary condition at $R > a_\xi$ [eq. 22]. Thus, an uncoupled pressure diffusion equation

$$\frac{\partial u}{\partial t}=c_f\nabla^2 u \quad where \quad c_f=kM\frac{K+\frac{3}{4}G_{eq}}{Mb^2+K+\frac{3}{4}G_{eq}} \quad (38)$$

can be achieved by replacing eq. 37 in eq. 32 in conjunction with equality

$$\frac{\partial u}{\partial t}=\frac{\partial \Delta p}{\partial t}, \tag{39}$$

where c_f is the fluid diffusivity coefficient.

In addition, the boundary conditions of the flow problem are defined for the face of the cylinder ($r = R$) and beyond the area of influence of the pore pressure, whose limit is expressed by a_u: the impermeability of the cylinder face (non-existent flow) [eq. 40]; the absence of flow and excess of pore pressure beyond the influence zone of the pore pressure [eq. 41 and eq. 42, respectively].

$$\partial u/\partial t=0 \quad at \quad r=R \quad \forall \quad t \tag{40}$$

$$\partial u/\partial t=0 \quad at \quad r\geq a_u \quad \forall \quad t \tag{41}$$

$$u=0 \quad at \quad r\geq a_u \quad \forall \quad t \tag{42}$$

The initial pore pressure distribution, an initial condition of the expansion model, is discussed in the next section.

The solution of equation 38 with the described boundary and initial condition [eq. 40 to 42] is presented by

$$u=f(x)=\sum_{n=1}^{\infty} C_n^*[\omega_n Y_0(\alpha_n r)]e^{-c_f\alpha_n^2 t}, \tag{43}$$

which defines a pore pressure distribution along the radius at any time (t_i), where:

$$C_n^*=\frac{\int_R^a u(r,t_i)[\omega_n Y_0(\alpha_n r)-J_0(\alpha_n r)]r\,dr}{\int_R^a[\omega_n Y_0(\alpha_n r)-J_0(\alpha_n r)]^2 r\,dr} \tag{44}$$

where J_0 and Y_0 are the zero order Bessel functions, of first and second kind, respectively. The variable α_n in the eq. 43 and 44 is given by the nth root of

$$Y_1(xR)J_0(x\alpha)-Y_0(x\alpha)J_1(xR)=0, \tag{45}$$

where ω_n is given by

$$\omega_n=-[Y_1(\alpha_n R)]/[J_1(\alpha_n R)]. \tag{46}$$

Thus, the excess of pore pressure (u) is a sum of n terms, each term obtained with the α_n value corresponding to nth root of the eq. 45; where J_1 and Y_1 are the first order Bessel functions, of first and second kind, respectively.

Through eq. 43 to 46 it is possible to compute excess pore pressure. Once computed it is possible to obtain the variation of the pore pressure, with $\Delta p = u - u_0$. The variation in pore pressure can then be replaced in eq. 31, making it possible to solve the differential equation and obtain displacements, stresses and strains.

2.4 Initial pore pressure distribution

Keeping in mind that the problem is restricted to small deformations and the expansion happens from an initial cylinder of radius R to a final diameter $R + \alpha R$. An initial disturbance of excess pore pressure was defined, a disturbance that would be caused by the initial insertion of the cylinder. This disturbance is applied in the so called influence zone, from $r = R$ to $r = a_u$.

In this sense, Randolph and Wroth [16] presented a distribution model of excess pore pressure caused by the insertion of piles and Morris and Willians [17] presents similar models, however related to the distribution of excess pore pressure caused by the insertion of the Vane Test equipment. Although, when confronting these propositions with the boundary conditions [eq. 47 to 50] it is noted that these models do not respect the cylindrical impermeability condition [eq. 49] nor the limit of the drainage zone [eq. 50]. Dienstmann [10] presents a proposal based on combinations of logarithmic and hyperbolic functions that guarantees compliance of the impermeability of the cylinder, however it still does not respect the boundary condition of the limit of the drainage zone [eq. 50].

$$u_0(r=R)=u_{0,max} \quad \text{Maximum pore pressure value on the face of the cylinder.} \tag{47}$$

$$u_0(r\geq a_u)=0 \quad \text{Limit of the initial zone influenced by poropressure excess.} \tag{48}$$

$$\partial u_0(r=R)/\partial t=0 \quad \text{Cylinder impermeability.} \tag{49}$$

$$\partial u_0(R\geq a_u)/\partial t=0 \quad \text{Limit of the drainage zone.} \tag{50}$$

On this matter, Forcelini [11] proposes eq. 51 and 52, a correction to the radial distribution model of excess initial pore pressure presented by Dienstmann [10], in this model all boundary conditions are satisfied.

$$u_0 = u_{0,max} \cdot \left[\frac{\frac{A}{r} + Br + \frac{a_p}{R} \ln\left(\frac{a_p}{r}\right) + C}{\frac{A}{R} + BR + \frac{a_p}{R} \ln\left(\frac{a_p}{R}\right) + C} \right] \quad in \quad R \le r \le a_u \tag{51}$$

where:

$$A = -a_p^2/(R+a_p); \quad B = a_p/[R(R+a_p)]; \quad C = a_p(R-a_p)/[R(R+a_p)] \tag{52}$$

Finally, the estimate of the maximum value of the pore pressure excess distribution ($u_{0,max}$), for sake of simplicity, can be based on the stress path of an undrained triaxial test:

$$u_{0,max} = (1/2)\sigma'_{0m}(1+M_{cs}) \tag{53}$$

where M_{cs} is the critical state line in the Cambridge space (p',q).

For a set of modeling, the equation proposed by Forcelini [eq. 51] was considered. The cavity expansion was performed at different rates (v) and the results of radial distribution of normalized pore pressure excess are shown in Fig. 3:

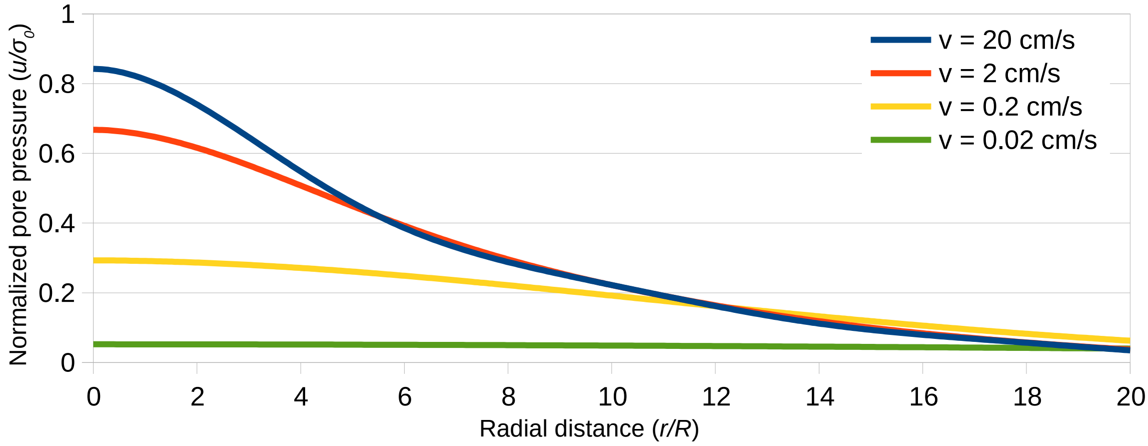

Figure 3. Radial distribution of normalized pore pressure excess for different rates.

3 Conclusions

In this work, a cylindrical cavity expansion model with semi-analytical solutions was presented. The model was developed in order to evaluate drainage behavior presented by the soil when submitted to field tests as CPTu. Preliminary results indicate the model's ability to represent the typical drainage behavior in the radial distance. Based on this model, parametric analyzes are being developed to identify parameters that influence the drainage curve.

Acknowledgements. The authors would like to thank the Federal University of Santa Catarina, for the institutional support and structure. Thanks also to the research funding institutions, CAPES and CNPq for their financial support. And last but not least, the authors would like to thank the entire research community in the area of knowledge.

Authorship statement. The authors hereby confirm that they are the sole liable persons responsible for the authorship of this work, and that all material that has been herein included as part of the present paper is either the property (and authorship) of the authors, or has the permission of the owners to be included here.

References

[1] M. A. BIOT. General theory of three-dimensional consolidation. *Journal of Applied Physics*, vol. 12, n. 2, pp. 155–164, 1941.
[2] R. Q. COUTINHO and F. C. MELLIA. Analysis of drainage conditions for intermediate soils from the piezocone tests. *Cone Penetration Testing*, p. 235–240, 2018.
[3] ASTM. Standard Test Method for Electronic Friction Cone and Piezocone Penetration Testing of Soils. Current, 2012.
[4] ABNT. NBR 12069 (Cancelled): Solo – Ensaio de penetração de cone in situ (CPT). Rio de Janeiro, 1991.
[5] F. SCHNAID AND E. ODEBRECHT. Ensaios de campo e suas aplicaçõs à engenharia. 2a ed. São Paulo: Oficina de Textos, 2012.
[6] J. A. SCHNAIDER, B. M. LEHANE, F. SCHNAID. Velocity Effects on Piezocone Meansurements in Normally an Over Consolidated Clays. *International Journal of Physical Modelling in eomechanics*, vol. 2, pp. 23–34, 2007.
[7]J. T. DEJONG and M. RANDOLPH. Influence of Partial Consolidation during Cone Penetration on Estimated Soil Behavior Type and Pore Pressure Dissipation Measurements. *Journal of Geotechnical and Geoenvironmental Engineering*, vol. 3, pp. 6–11, 2011.
[8] R. SALGADO, M. PREZZI. Penetration Rate Effects on Cone Resistance : Insights From Calibration Chamber and Field Testing. *Soils and Rocks*, vol. 37, n. 3, pp. 233–242, 2015.
[9] G. E. BLIGHT. A note on field vane testing of silty soils. *Canadian Jeotechnical journal*, vol. 3, pp. 143–149, 1968.
[10]DIENSTMANN, G. Análise de Ensaios de Campo em Fluxo Transitório. Tese de Doutorado. Universidade Federal do Rio Grande do Sul. 2015.
[11]FORCELINI, M. Modelagem em poroelasticidade não linear do ensaio de palheta em rejeitos de mineração. Dissertação de mestrado. Universidade Federal do Rio Grande do Sul. 2019.
[12] K. KIM, M. PREZZI, R. SALGADO, W. LEE. Effect of Penetration Rate on Cone Penetration Resistance in Saturated Clayey Soils. *Journal of Geotechnical and Geoenvironmental Engineering*, vol. 134, n. 8, pp. 1142–1153, 2008.
[13] S. F.CHUNG, M. F. RANDOLPH, J. ASCHNEIDER. Effect of Penetration Rate on Penetrometer Resistance in Clay. *Journal of Geotechnical and Geoenvironmental Engineering*, vol. 132, n. 9, ppp. 1188–1196, 2006.
[14] Y. Suzuki and B.M. Lehane. Analysis of CPT end resistance at variable penetration rates using the spherical cavity expansion method in normally consolidated soils. *Computers and Geotechnics*, vol. 69, pp. 141–152, 2015.
[15] S. Maghous, L. Dormieux, and J. Barthéléemy. Micromechanical approach to the strength properties of frictional geomaterials. *Eur. J. Mech. A/Solids*, vol. 28, pp. 179–188, 2009.
[16] M. F. RANDOLPH and C. P. WROTH. An analytical solution for the consolidation around a driven pile. *International Journal for Numerical and Analytical Methods in Geomechanics*, vol. 3, pp. 217–229, 1979.
[17] P. H. MORRIS and D. J. WILLIAMS. A revision of Blight's model of field vane testing. *Canadian Geotechnical Journal*, vol. 37, n. 5, pp. 1089–1098, 2000.